07

UV detectors based on Ga_2O_3 films with high-speed performance

© D.A. Almaev,[1,2] A.V. Tsymbalov,[1] V.V. Kopyev[1]

[1] Tomsk State University,
634050 Tomsk, Russia
[2] Tomsk State University of Control Systems and Radioelectronics,
634050 Tomsk, Russia
e-mail: almaev001@mail.ru

Received March 26, 2025
Revised May 6, 2025
Accepted June 30, 2025

The paper presents a study of the influence of annealing temperature in an Ar atmosphere and growth time of gallium oxide films on the electrical and photoelectric characteristics of Pt/Ga_2O_3 structures. Gallium oxide films were obtained by RF-magnetron sputtering on sapphire substrates with the base orientation (0001). Ga_2O_3 films are characterized by high transparency in the long-wave UV (UVA) and visible (VIS) ranges $T > 80\,\%$. The maximum photosensitivity value corresponds to structures annealed at $900\,^\circ$C with an active region thickness of $d = 190$ nm. The values of responsivity and photo-to-dark current ratio were 134 mA/W and $5.2 \cdot 10^5$ a. u, respectively, at a voltage of 100 V. The structures are characterized by high speed-performance, the shortest response and recovery times at a voltage of 10 V were 2.1 ms and 0.6 ms, respectively.

Keywords: photodetector, gallium oxide, RF-magnetron sputtering, UV radiation, speed- performance.

DOI: 10.61011/TP.2025.11.62243.49-25

Introduction

Gallium oxide (Ga_2O_3) belongs to the class of ultra-wide-band semiconductors n, a type of conductivity with a band gap in the range $E_g = 4.4-5.3$ eV. Ga_2O_3 has unique physico-chemical properties that meet the requirements of modern micro- and optoelectronics [1,2]. This material demonstrates polymorphism and can exist in five crystalline modifications: α, β, γ, δ and $\varepsilon(\kappa)$. The β-phase, characterized by a monoclinic crystal lattice, high chemical inertia and thermal stability, is the most studied, which makes it promising for applications in devices operating under extreme conditions [3].

Due to its unique properties Ga_2O_3 is widely used in various technological fields, including power electronics, gas sensors, transparent electrodes and UV detectors [4]. Of particular interest is the development of UV photodetectors based on Ga_2O_3, due to its high band gap, selectivity, and the effect of internal amplification [5]. Among the known design solutions, the most widespread are metal-semiconductor-metal (MSM) planar structures, which are characterized by high sensitivity and technological simplicity [6].

The electrical and photoelectric characteristics of such detectors are largely determined by the methods of growth and subsequent processing of structures based on Ga_2O_3 [7]. Currently, gallium oxide films are formed by various technological methods, including pulsed laser deposition (PLD), molecular beam epitaxy (MBE), deposition of organometallic compounds from the gas phase (MOCVD), chemical gas-phase deposition under reduced pressure (LPCVD), chloride vapor-phase epitaxy (HVPE), atomic layer deposition (ALD) and RF magnetron sputtering (RFMS) [3,8]. The latter method attracts attention due to the high growth rate of films and the cost-effectiveness of production, while the formed structures are highly sensitive to UV radiation.

The optical and photoelectric characteristics of the structures directly depend on the technology of producing gallium oxide films, as well as subsequent operations. In this regard, this paper is aimed at studying the effect of growth time and annealing temperature conditions of Ga_2O_3 films on the optical, electrical, and photoelectric properties of Pt/Ga_2O_3 structures.

1. Research methodology

Films Ga_2O_3were obtained by the RFMS target method Ga_2O_3 (99.999 %) on smooth sapphire substrates on the AUTO-500 (Edwards) installation in the gas mixture Ar/O_2. The films were sputtered during $t_g = 30$ and 60 min. The oxygen concentration in the mixture was maintained at (56.1 ± 0.5) vol.%. The distance between the target and the substrate was 70 mm. The pressure in the chamber during spraying was maintained at $7 \cdot 10^{-6}$ bar. There was no deliberate doping of films during the growth process. At the next stage, the substrate was divided into several parts, which were then annealed in an argon stream at temperatures of $T_{an} = 700\,^\circ$C, $800\,^\circ$C and $900\,^\circ$C for 30 min. Further, Pt contacts with a counter-pin topology with an interelectrode distance of $l = 200\,\mu$m were formed on the surface of the films Ga_2O_3m. Sapphire plates with Ga_2O_3 film and Pt contacts were cut into individual samples of size 0.3×0.3 cm. Six series of samples with different growth times and annealing temperatures were obtained as

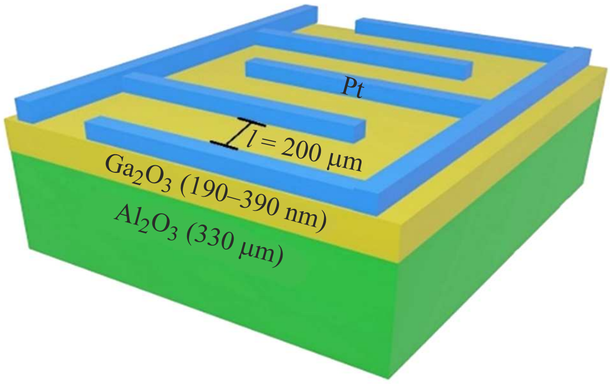

Figure 1. Schematic representation of the Pt/Ga_2O_3 structure.

a result. A schematic representation of the MSM structures of Pt/Ga_2O_3 is shown in Fig. 1.

The X-ray diffraction analysis (XDA) method was used to determine the phase composition of the films. The measurements were carried out using an X'PERT PRO diffractometer manufactured by PANalytical with radiation CuK_α ($\lambda = 1.5406$ Å) at a voltage of 40 kV and a current of 30 mA.

A deuterium lamp D-2000 Micropack was used as a radiation source for measuring transmission spectra, providing stable radiation in the range of $\lambda = 190 - 400$ nm. The transmitted radiation entered the input of the Ocean Optics Flame spectrometer with an operating range of $\lambda = 200 - 850$ nm. The measurement of λ was carried out with an optical resolution of 1 nm. The measurements were controlled using the OceanView software.

Measurements of volt-ampere characteristics (VAC) in dark conditions and under illumination were carried out using a Nextron microprobe installation and a Keithley 2636A measuring source. A krypton-fluorine lamp with a radiation flux density of $P = 780\,\mu$W/cm^2 was used as a source of monochromatic ($\lambda = 254$ nm) radiation.

The photo I_{ph} to dark current ratio I_D (PDCR), current monochromatic sensitivity R_λ, specific detection ability D^*, and quantum efficiency η were calculated using the following expressions [5]:

$$\text{PDCR} = I_{ph}/I_D, \quad (1)$$

$$R_\lambda = I_{ph}/(P \cdot S_{\text{eff}}), \quad (2)$$

$$D^* = R_\lambda \cdot (S_{\text{eff}}/(2 \cdot e \cdot I_D))^{1/2}, \quad (3)$$

$$\eta = R_\lambda \cdot h \cdot c/(e \cdot \lambda), \quad (4)$$

where S_{eff} is the effective area of the irradiated surface of the photodetector; e is the electron charge; h is the Planck's constant; c is the speed of light in a vacuum.

The pulse characteristics of the detectors were measured using a Tektronix 104XS digital oscilloscope with a bandwidth of 1 GHz and a UV LED with a maximum intensity of $\lambda = 255$nm.

The rise time of the photocurrent t_r is defined as the time during which the current increases from 10 % to 90 % of the maximum value under irradiation. The photocurrent decay time t_f is defined as the time during which the current decreases from 90 % to 10 % of the maximum value after exposure to radiation.

2. Results and discussion

Diffraction patterns of Ga_2O_3 films (Fig. 2) show multiple peaks corresponding to reflections from planes (−110), (−311), (−603), (−221) and (603), which refer to β-Ga_2O_3. The position of the peaks and their intensity are practically independent of the annealing temperature. All diffraction patterns contain peaks from the sapphire substrate corresponding to the family of planes (0001). The XDA showed that all Ga_2O_3 films are polycrystalline and correspond to the β-phase.

Fig. 3 shows the optical transmission spectra of Ga_2O_3 films before and after annealing in an Ar atmosphere for different T_{an}. To determine the thickness of the films d, an expression for the transmittance coefficient T was used, taking into account multiple reflections inside the sample and interference of rays exiting the sample [9]. The thickness of Ga_2O_3 films was 190 and 390 nm for $t_g = 30$ and 60 min, respectively. The values of T decrease with an increase of t_g by almost two times, which corresponds to a change of d. In addition, the ratio $\alpha d \approx 1$ is fulfilled, where α is the absorption coefficient, which indicates the absence of strong absorption.

The dependence of α on the photon energy $h\nu$ was studied to determine the value of the optical band gap E_g^{opt}. More precisely, this dependence is approximated in coordinates $(\alpha h\nu)^2$ from $h\nu$, which indicates direct optical transitions, and the values of E_g^{opt} for films Ga_2O_3 were $4.82 - 4.92$ eV, which corresponds to the literature

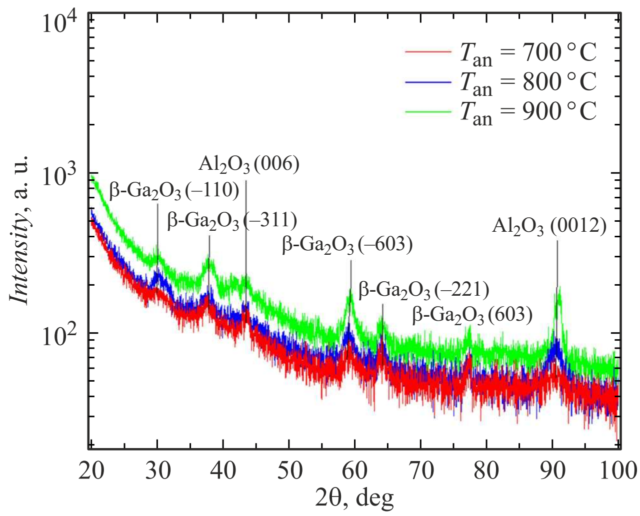

Figure 2. XDA spectra of Ga_2O_3 films on sapphire substrates annealed at different temperatures.

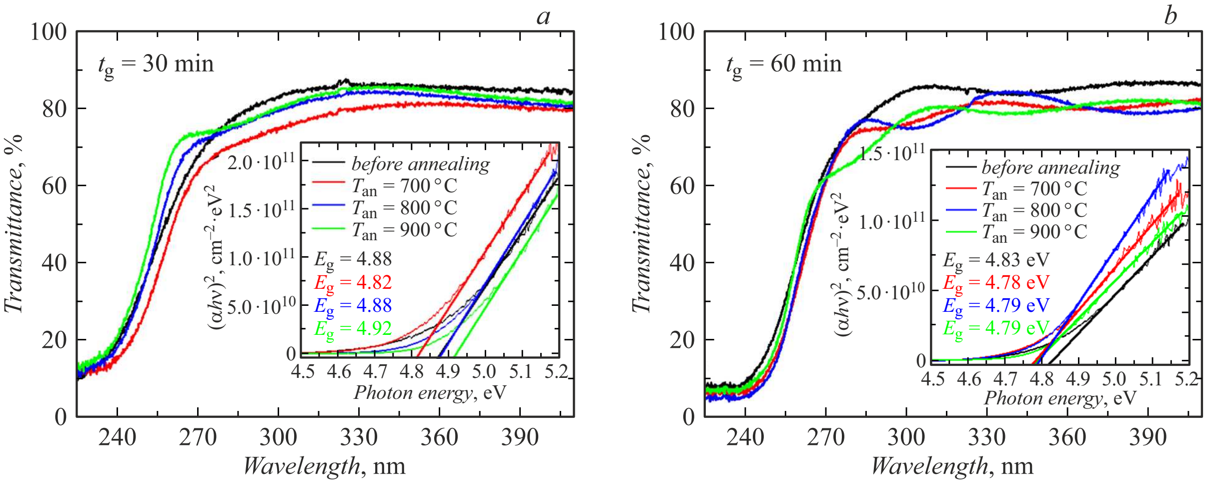

Figure 3. Optical transmission spectrum of films of β-Ga_2O_3 for $t_g = 30$ and 60 min at different T_{an} in argon. Insert — dependence of $(\alpha h\nu)^2$ on the photon energy.

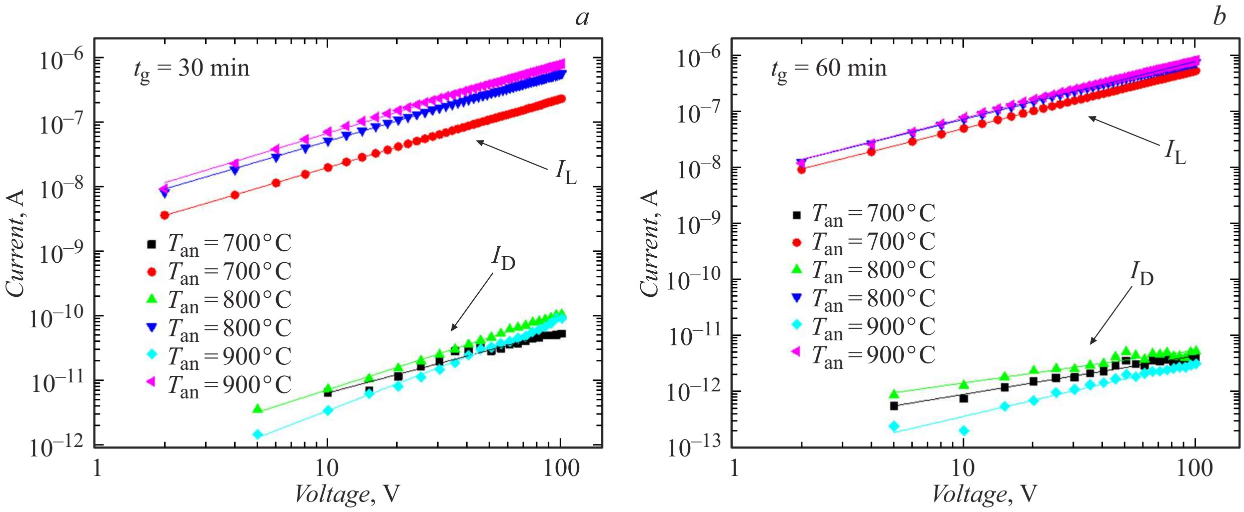

Figure 4. VAC of structures of Pt/β-Ga_2O_3 in dark conditions and when exposed to UV radiation.

Table 1. Values of the exponent m for thin films Ga_2O_3

t_g, min		30			60		
T_{an}, °C		700	800	900	700	800	900
m	I_D	0.96 ± 0.06	1.16 ± 0.01	1.39 ± 0.02	0.69 ± 0.03	0.58 ± 0.03	0.96 ± 0.05
	I_L	1.06 ± 0.01	1.05 ± 0.01	1.09 ± 0.01	1.03 ± 0.01	1.03 ± 0.01	1.05 ± 0.01

data [4]. The values of E_g^{opt} vary within the margin of error (± 0.05 eV).

Fig. 4 shows the VAC of Pt/Ga_2O_3 structures. The dependence of I_D on U is linear ($I_D \propto U^m$, where $m \approx 1$ (Table. 1)) and symmetrical with respect to the polarity of the applied voltage. Small deviations from the linearity of the values I_D are caused by their small magnitude, which are in the lower limit of the measuring equipment. The values of I_D for Pt/Ga_2O_3 structures do not exceed 100 pA at $U = 100$ V, and the conductivity is determined by Ohm's law in the considered electric fields. Exposure to UV radiation from $\lambda = 254$ nm leads to an increase in current by 4–5 orders of magnitude. The change in photosensitivity is most noticeable for thinner films, the values of the total current under illumination I_L increase from 9 to 780 nA in the voltage range from 0 to 100 V. The values of I_L increase from 120 to 850 nA in the same voltage range for photodetectors with 390 nm thick Ga_2O_3 films. At the same time, the greatest photosensitivity is typical for structures based on thicker films, which is associated with higher

Table 2. Values of photovoltaic characteristics of structures Pt/Ga_2O_3 at $U = 100$ V

t_g, min	30			60		
T_{an}, °C	700	800	900	700	800	900
I_D, pA	54	106	92	4.4	5.4	3.3
PDCR, a.u.	$8.6 \cdot 10^3$	$1.1 \cdot 10^4$	$1.7 \cdot 10^4$	$2.4 \cdot 10^5$	$2.8 \cdot 10^5$	$5.2 \cdot 10^5$
R_λ, mA/W	36	88	124	86	124	134
η, %	17.5	42.8	60.8	42.2	60.4	65.6
D^*, cm·$Hz_{0.5}$/W	$1.5 \cdot 10^{11}$	$2.7 \cdot 10^{11}$	$4.2 \cdot 10^{11}$	$7.5 \cdot 10^{11}$	$1.7 \cdot 10^{12}$	$2.5 \cdot 10^{12}$

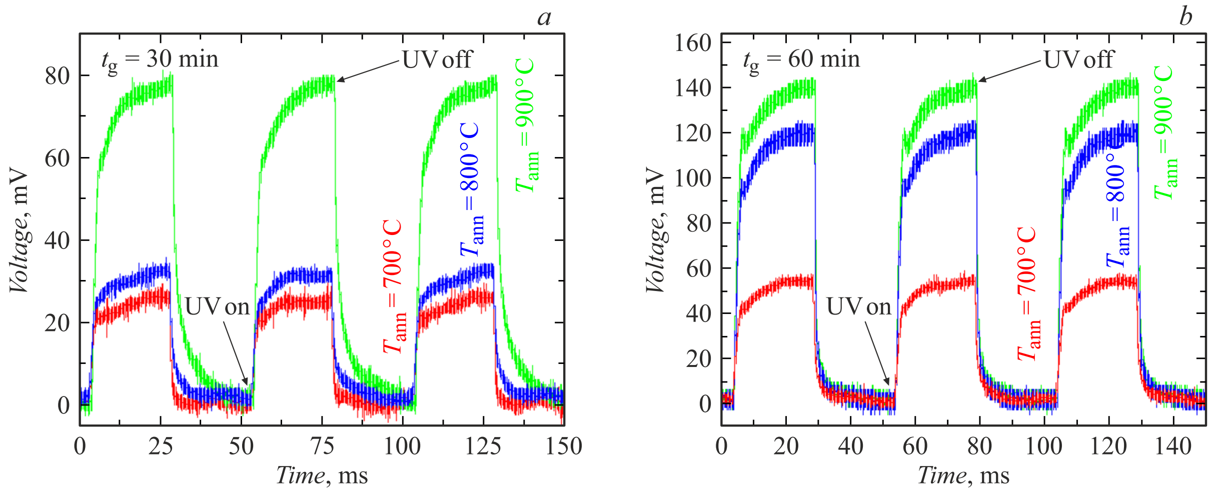

Figure 5. Waveforms of Pt/β-Ga_2O_3 structures under pulsed exposure to a UV light emitting diode with $\lambda = 255$ nm.

absorption of UV radiation. It is worth noting the absence of the classical [7,8] for Ga_2O_3 photoconductivity saturation, which limits operation over a wide voltage range.

The main photovoltaic characteristics were calculated from the VAC analysis, which are compared for all series of samples in Table 2. The values of R_λ increase with the growth of t_g and T_{an}. The greatest effect of film thickness on R_λ is observed at lower values of T_{an}, at $T_{an} = 900$ °C, the values of R_λ are almost identical, but the values of PDCR and D* vary by more than an order of magnitude, which is related to the change I_D.

The performance of photodetectors based on Pt/Ga_2O_3 structures at $U = 10$ V was determined using the waveforms shown in Fig. 5. The values of t_r and t_f are compared in Table 3. It can be seen from the data presented

Table 3. Values of time constants t_r and t_f for structures of Pt/Ga_2O_3 at $U = 10$ V

t_g, min	30			60		
T_{an}, °C	700	800	900	700	800	900
t_r, ms	2.1	5.0	7.2	5.9	5.5	6.1
t_f, ms	0.6	3.8	5.9	1.6	1.4	2.7

that there is a relationship between photosensitivity and the performance [10]. The structures of Pt/Ga_2O_3 are characterized by high stability and repeatability of characteristics in the pulsed mode, there is no pronounced residual photoconductivity, as was shown earlier [10, 11]. The speed should be understood as the sum of t_r and t_f, which does not exceed 10 ms and determines the maximum frequency of pulse reception by the photodetector without taking into account auxiliary electronics.

The results of the study of the photovoltaic characteristics of Pt/Ga_2O_3 structures obtained in this work can be compared with previously published data from Ref. [12–18] (Table 4). High values of I_D are observed in several studies, which leads to a low PDCR [15,16,18].

An increase in T_{an} films Ga_2O_3 leads to an increase in the quantum efficiency of Pt/Ga_2O_3 structures, which is due to the photoresistive amplification mechanism, the essence of which is an increase in time the lives of the main carriers. This is explained by the fact that an increase in the annealing temperature Ga_2O_3 improves the quality of the film, thereby leading to a decrease in the concentration of initial defects in the volume of the gallium oxide film, which were responsible for the recombination of the main charge carriers. In addition, with a high annealing temperature, new defects appear that can contribute to

Table 4. Photovoltaic characteristics of MSM photodetectors based on Ga2O3 films obtained by RFMS

Structure	Au/Pt/Ti/Ga_2O_3	Au/Ti/Ga_2O_3				Al/Ga_2O_3	Al/Ga_2O_3
λ, nm	254						
I_D, nA	–	$82 \cdot 10^{-6}$	$7 \cdot 10^{-3}$	4	0.1	$66.2 \cdot 10^{-3}$	$3 \cdot 10^3$
I_{ph}, μA	57	$3 \cdot 10^{-2}$	6.5	21	0.1	$27.7 \cdot 10^{-3}$	1.5
PDCR, a.u.	–	$3.6 \cdot 10^5$	$9.4 \cdot 10^5$	$5.3 \cdot 10^3$	$1 \cdot 10^3$	419	0.5
R_λ, A/W	48.9	1.9	8.6	46.3	–	$0.8 \cdot 10^{-3}$	20
η, %	$2.4 \cdot 10^4$	927.2	$4.2 \cdot 10^3$	$2.2 \cdot 10^4$	–	0.4	$1 \cdot 10^4$
D^*, cm·$Hz_{0.5}$/W	$1.4 \cdot 10^{14}$	$6.5 \cdot 10^{13}$	$1.6 \cdot 10^{12}$	$1.8 \cdot 10^{13}$	–	–	–
t_r, ms	118	–	390	2820	1830	38680	15200
t_f, ms	31	–	124	320	960	3980	53500
Source	[12]	[13]	[14]	[15]	[16]	[17]	[18]

photoconductivity, such as oxygen vacancies, which are formed during annealing in an inert medium [19]. Oxygen vacancies probably contribute more to the conductivity of thinner films, which is manifested in higher values of I_D [20–22]. An increase in the thickness of Ga_2O_3 film leads to an increase in current monochromatic sensitivity due to higher absorption in the active region of the structure.

The condition of low I_D and high PDCR is one of the key conditions in real-world photodetector operation. The values R_λ and η characterize the photosensitivity of the photodetector and often significantly exceed the theoretical maximum for Ga_2O_3, which is associated with the internal gain in this material. In most cases, photosensitivity is determined by the interelectrode distance, type and topology of the metal contact, which allows it to be controlled over a wide range. Most often, metal contacts are located at a distance of units and tens μm [6,7]. This paper studied the performance of photodetectors based on Ga_2O_3 films, therefore structures with a relatively large interelectrode distance were used, which significantly improved the performance and overall quality of photodetectors, while avoiding early saturation of the photoconductivity by voltage.

Conclusion

The photoelectric characteristics of photodetectors based on Pt/Ga_2O_3 structures obtained by RF magnetron sputtering were studied in this paper. The influence of the film growth time and annealing temperature on the optical and electrical properties of the structures is analyzed. It has been found that an increase in the thickness of Ga_2O_3 films leads to an increase in photosensitivity, which is associated with an increase in the absorption coefficient in the UV range. The analysis of the VAC showed that the structures of Pt/Ga_2O_3 demonstrate a linear dependence of current on voltage and a significant increase in current when exposed to UV radiation. Photodetectors have high stability and repeatability of characteristics under pulsed illumination by a emitting LED, which makes them promising for use in high-speed detection systems. A comparison of the data obtained with literary sources has shown that the studied structures have competitive characteristics, including high sensitivity and high performance. The revealed possibility of controlling photovoltaic parameters due to film thickness and annealing temperature opens up prospects for further optimization of structures for practical use in new generation UV detectors.

Funding

The study was carried out with the support of the Tomsk State University Development Program (Priority 2030), project No.2.5.4.25 ML.

Conflict of interest

The authors declare that they have no conflict of interest.

References

[1] Z. Fei, Z. Chen, W. Chen, S. Chen, Z. Wu, X. Lu, G. Wang, J. Liang, Y. Pei. J. Alloys Compounds, **925**, 166632 (2022). DOI: 10.1016/j.jallcom.2022.166632
[2] J.A. Spencer, A.L. Mock, A.G. Jacobs, M. Schubert, Y. Zhang, M.J. Tadjer. Appl. Phys. Rev., **9**, 011315 (2020). DOI: 10.1063/5.0078037
[3] T. Zhao, H. He, C. Wu, L. Lai, Y. Ma, H. Yang, H. Hu, A. Liu, D. Guo, S. Wang. ACS Appl. Nano Mater., **6** (5), 3856 (2023). DOI: 10.1021/acsanm.2c05499
[4] S.J. Pearton, J. Yang, P.H. Cary, F. Ren, J. Kim, M.J. Tadjer, M.A. Mastro. Appl. Phys. Rev., **5** (1), 011301 (2018). DOI: 10.1063/1.5006941
[5] D. Kaur, M. Kumar. Adv. Opt. Mater., **9** (9), 2002160 (2021). DOI: 10.1002/adom.202002160

[6] H. Zhai, Z. Wu, Z. Fang. Ceram. Intern., **48** (17), 24213 (2022). DOI: 10.1016/j.ceramint.2022.06.066
[7] X. Chen, F. Ren, S. Gu, J. Ye. Photon. Res., **7** (4), 381 (2019). DOI: 10.1364/PRJ.7.000381
[8] X. Hou, Y. Zou, M. Ding, Y. Qin, Z. Zhang, X. Ma, P. Tan, S. Yu, X. Zhou, X. Zhao, G. Xu, H. Sun, S. Long. J. Phys. D: Appl. Phys., **54** (4), 043001 (2020). DOI: 10.1088/1361-6463/abbb45
[9] T.S. Moss, G.J. Burrell, B. Ellis. *Semiconductor Opto-Electronics* (Halsted Press Division, Wiley, 1973), p. 441.
[10] V.M. Kalygina, A.V. Tsymbalov, P.M. Korusenko, A.V. Koroleva, E.V. Zhizhin. Crystals, **14** (3), 268 (2024). DOI: 10.3390/cryst14030268
[11] V. Kalygina, A. Tsymbalov, A. Almaev, Ju. Petrova, S. Podzyvalov. Physica Status Solidi B: Basic Res., **259** (2), 2100341 (2021). DOI: 10.1002/pssb.202100341
[12] X. Gao, T. Xie, J. Wu, J. Fu, X. Gao, M. Xie, H. Zhao, Y. Wang, Z. Shi. Appl. Phys. Lett., **125** (17), 172103 (2024). DOI: 10.1063/5.0227397
[13] S. Zhou, X. Peng, H. Liu, Z. Zhang, L. Ye, H. Li, Y. Xiong, L. Niu, F. Chen, L. Fang, C. Kong, W. Li, X. Yang, H. Zhang. Opt. Mat. Expr., **12** (1), 327 (2022). DOI: 10.1364/OME.449496
[14] L. Li, C. Li, S. Wang, Q. Lu, Y. Jia, H. Chen. J. Semiconductors, **44** (6), 062805 (2023). DOI: 10.1088/1674-4926/44/6/062805
[15] M. He, Q. Zeng, L. Ye. Crystals, **13** (10), 1434 (2023). DOI: 10.3390/cryst13101434
[16] J. Wang, L. Ye, X. Wang, H. Zhang, L. Li, C. Kong, W. Li. J. Alloys Compounds, **803**, 9 (2019). DOI: 10.1016/j.jallcom.2019.06.224
[17] C. Wang, W.-H. Fan, Y.-C. Zhang, P.-C. Kang, W.-Y. Wu, D.-S. Wuu, S.-Y. Lien, W.-Z. Zhu. Ceram. Intern., **49** (7), 10634 (2023). DOI: 10.1016/j.ceramint.2022.11.251
[18] K. Arora, N. Goel, M. Kumar, M. Kumar. ACS Photonics, **5** (6), 2391 (2018). DOI: 10.1021/acsphotonics.8b00174
[19] A.Y. Polyakov, E.B. Yakimov, I.V. Shchemerov, A.A. Vasilev, A.I. Kochkova, V.I. Nikolaev, S.J. Pearton. J. Phys. D: Appl. Phys., **58** (6), 063002 (2025). DOI: 10.1088/1361-6463/ad8e6e
[20] S. Cui, Z. Mei, Y. Zhang, H. Liang, X. Du. Adv. Opt. Mat., **5** (19), 1700454 (2017). DOI: 10.1002/adom.201700454
[21] C. Zhou, K. Liu, X. Chen, J. Feng, J. Yang, Z. Zhang, L. Liu, Y. Xia, D. Shen. J. Alloys Compounds, **840**, 155585 (2020). DOI: 10.1016/j.jallcom.2020.155585
[22] A. Almaev, V. Nikolaev, V. Kopyev, S. Shapenkov, N. Yakovlev, B. Kushnarev, A. Pechnikov, J. Deng, T. Izaak, A. Chikiryaka, M. Scheglov, A. Zarichny. IEEE Sensors J., **23** (17), 19245 (2023). DOI: 10.1109/JSEN.2023.3297127

Translated by A.Akhtyamov